ARTICLE

A Mechanism Study of a Novel Acid-Activatable Michael-Type Fluorescent Probe for Thiols

Yao Tong[a], Chun-guang Dai[a], Yi Ren[b], Shi-wei Luo[a]*

a. Department of Chemistry, University of Science and Technology of China, Hefei 230026, China
b. College of Chemistry and State Key Laboratory of Biotherapy, Sichuan University, Chengdu 610064, China

(Dated: Received on December 24, 2014; Accepted on April 14, 2015)

A Michael addition is usually taken as a base-catalysed reaction. However, our synthesized 2-(quinolin-2-ylmethylene) malonic acid (QMA) as a Michael-type thiol fluorescent probe is acid-active in its sensing reaction. In this work, based on theoretic calculation and experimental study on 7-hydroxy-2-(quinolin-2-ylmethylene) malonic acid, we demonstrated that QMA as a Michael acceptor is acid-activatable, *i.e.*, it works only in solutions at pH<7, and the lower the pH of solutions is, the higher reactivity QMA has. In alkaline solution, the malonate QMA[-2H$^+$]$^{2-}$ cannot react with both RS$^-$ and RSH. In contrast, 2-(quinolin-2-ylmethylene) malonic ester (QME), the ester of QMA, reveal a contrary pH effect on its sensing reaction, that is, it can sense thiols in alkaline solutions but not in acidic solutions, like a normal base-catalysed Michael addition. The values of activation enthalpies from theoretic calculation support the above sensing behavior of two probes under different pH conditions. In acidic solutions, the protonated QMA is more highly reactive towards electrophilic attack over its other ionized states in neutral and alkaline solutions, and so can react with lowly reactive RSH. In contrast, there is a big energy barrier in the interaction of QME with RSH (acidic solutions), and the reaction of QME with the highly reactive nucleophile RS$^-$ is a low activation energy process (in alkaline solutions). Theoretic calculation reveals that the sensing reaction of QMA undergoes a 1,4-addition process with neutral thiols (RSH), and a 1,2-addition pathway for the sensing reaction of QME with RS$^-$. Therefore, the sensing reaction of QMA is an acid-catalysed Michael addition via a 1,4-addition, and a normal base-catalysed Michael addition via a 1,2-addition.

Key words: Fluorescent probe, Thiols, Michael addition, DFT calculation, Transition state, Activation enthalpy

I. INTRODUCTION

Thiols is an important class of molecules in biological systems and chemical science. Several aliphatic thiols including cysteine (Cys), homocysteine (Hcy) and glutathione (GSH) play essential roles in many physiological processes [1]. For example, GSH is critical in maintaining redox homeostasis [2], which is important for the maintenance of cellular defense against reactive oxygen species and for a number of biological processes. Abnormal levels of cellular thiols are associated with many human diseases, such as slow growth, hair depigmentation, edema, lethargy, liver damage, loss of muscles and fat, skin lesions, weakness [3], cardiovascular diseases and Alzheimer's disease [4]. Therefore, selective detection of cellular biothiols is of growing importance.

Optical approaches based on synthetic colorimetric and fluorescent molecular probes have attracted increasing interest due to their simplicity, inexpensiveness, sensitivity and selectivity during the last decade [5]. A variety of colorimetric and fluorescent probes for thiols have been constructed by exploiting the high nucleophilic reactivity or transition metal-affinity of the thiol group, which involve specific reactions between probes and thiols, such as Michael addition [6], cleavage reactions by thiols [7], cyclization with aldehyde [8], metal complexes-displace coordination [9], and others [10]. Among these probes, the most cases involve the electrophilic reactivity of probe molecules and the nucleophilicity of thiols, such as the probes via Michael addition or aromatic nucleophilic substitution (S_NAr). Because the thiolate anion RS$^-$ is more nucleophilic than its neutral form, RSH (pK_a≈8.5), most fluorescent probes were designed to detect thiols in slight alkaline solutions (pH=7.2−9), which is the so-called physiological condition, for the real nucleophile is the thiolate anion RS$^-$. In other words, these thiol probes couldn't

*Author to whom correspondence should be addressed. E-mail: luosw@ustc.edu.cn

 ©2015 Chinese Physical Society

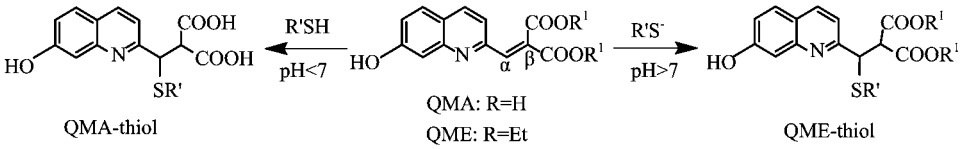

Scheme 1 Two fluorescent probes, QMA and QME, that response to thiols in different pH range of solutions.

work in acidic solutions. A few probes that can detect thiols at low pH (<6) were reported, but they are more active in alkaline solutions [11]. Recently, we found one kind of acid-activatable fluorescent probe for thiols, 2-(quinolin-2-ylmethylene) malonic acids (QMA), which can label lysosomes in live cells by the sensing reaction with biothiols [12]. This kind of fluorescent probes can detect thiols only in acidic solutions (pH<7), giving colorimetric and fluorescent response, but not in alkaline solutions (pH>7), shown in Scheme 1. In contrast, its ester QME displays a contrary pH effect on the sensing reactivity, which can act only at pH>7, as most Michael-type thiol probes reported [6].

To further understand two kinds of sensing reactions, we performed an experimental investigation and a theoretic study for the sensing reactions of various ionized-states of QMA or QME with several thiols (Fig.1) at B3LYP level of theory with Gaussian 09 program suite [13]. Two different sensing mechanisms have been demonstrated, that is, the sensing reaction of QMA is an acid-catalysed Michael reaction with RSH via 1,4-addition process, and the behavior of QME is a base-catalysed Michael reaction with RS^- via a 1,2-addition.

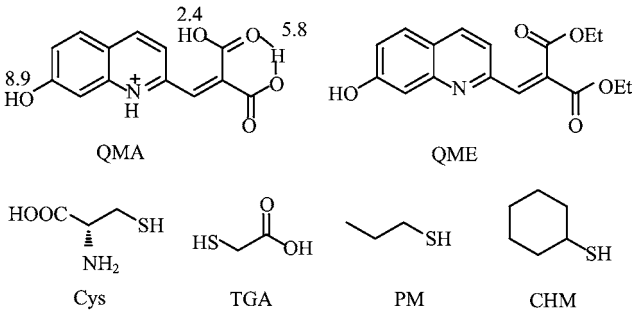

FIG. 1 Chemical structures of QMA, QME, and four kinds of thiols in this investigation.

II. EXPERIMENTAL AND THEORETICAL DETAILS

A. Materials and methods

The spectral measurements for obtaining pK_a values were performed in aqueous solutions at various pH ranges, which were DMSO/water (4:96, volume ratio) solvent mixture with four buffers over a pH range of 2−11, involving 0.1 mol/L critric acid-0.1 mol/L disodium hydrogen phosphate buffer for pH=2−5, 0.1 mol/L HAc-0.1 mol/L NaAc buffer for pH=5−5.5, 0.1 mol/L Na_2HPO_4-0.1 mol/L NaH_2PO_4 for pH=6−8 and 0.1 mol/L K_2CO_3-0.1 mol/L $NaHCO_3$ buffer for pH>8. Water for sample preparation was purified with a Millipore water system. All pH values of solutions were further measured with a MQK-PHS-3C pH meter.

Time-dependent response of QMA to different excess thiols exhibits pseudo-first-order reaction conditions. The rate constant k_{obs} is obtained according to the equation,

$$\ln\frac{A-A_{min}}{A_0-A_{min}} = -k_{obs}t \quad (1)$$

where A_0, A and A_{min} are absorption values at certain wavelength, where thiols have no absorption, of the solution before and after addition of thiols, and the corresponding adduct or after complete reaction of probe molecules, respectively. Furthermore, a second-order rate constant k was obtained according to the equation, k_{obs}=k[RSH], where [RSH] is the concentration of thiols.

B. Computational

All electronic structure optimization and frequency calculations were carried out using Gaussian 09 program suite [20]. The gas phase geometries of all compounds were optimized using the B3LYP density functional and the 6-31+G(d) basis set, without any structural constrains. Harmonic force constants were computed at the optimized geomeries to characterize the stationary point as minima or saddle points. Meanwhile, intrinsic reaction coordinate (IRC) calculations were performed to verify the transition states (TS) associated with the correct reactant and product. For compounds that have multiple conformations, efforts were made to find the lowest energy conformation by comparing the structures optimized from different starting geometries.

Enthalpy and Gibb's free energy corrections were obtained using unscaled frequencies and gas-phase enthalpy and Gibb's free energy changes were then obtained based on the frequency calculation. The electrostatic potential maps were drawn based on the optimized structures. UV-Vis absorption spectra were modified by using PBEPBE/6-31+G(d) method.

To examine the solvent effect, self-consistent reaction

DOI:10.1063/1674-0068/28/cjcp1412217 ©2015 Chinese Physical Society

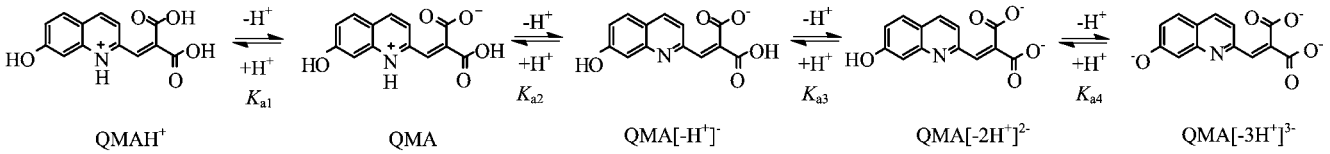

Scheme 2 Five ionization forms of QMA and equilibria between different ionization forms.

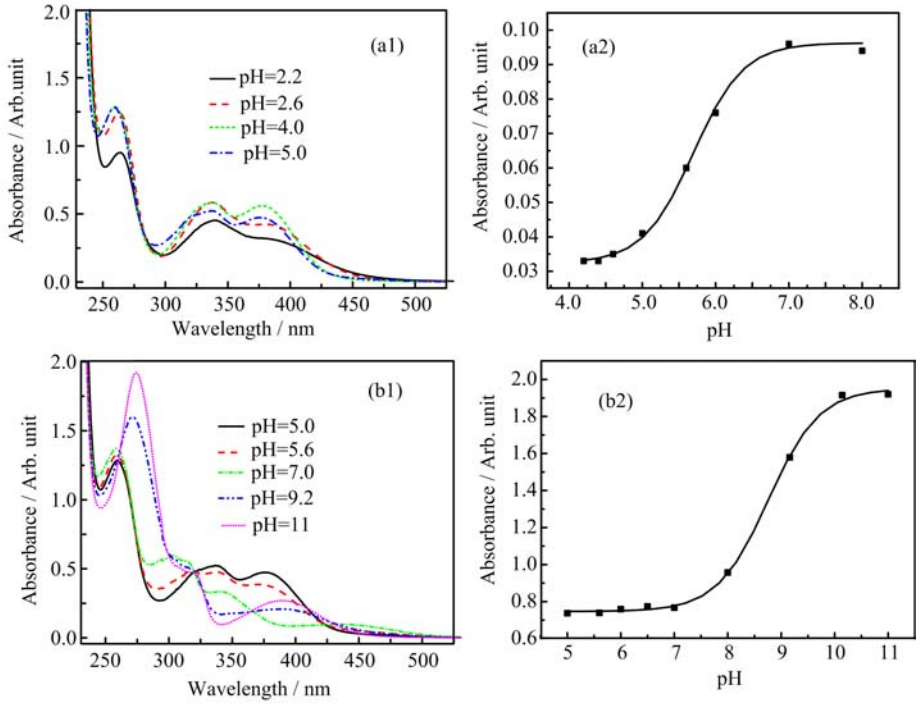

FIG. 2 UV-Vis absorption spectra of (a1, b1) QMA in various pH solutions and (a2, b2) QME in a pH=7.4 buffer solution.

field method with the conductor-like polarizable continuum model (C-PCM) solvation model was utilized. Water was chose as the solvent since the solvent was used in the experimental study. B3LYP functions combined with a lager basis set 6-311++G(d,p) were used to calculate the single point energies in water. The enthalpies and Gibb's free energies in water solution were obtained from the single point calculations, and the gas-phase enthalpy and Gibb's free energy corrections were included. We have used the enthalpy and Gibb's free energies obtained from the B3LYP/6-311++G(d,p)//B3LYP/6-31+G(d,p) calculations in water throughout the paperunless otherwise stated. All the thermodynamic calculations were performed at 25 °C and 1 atm.

III. RESULTS

A. Measurement of pK_a of QMA and ionized states of QMA

To measure pK_a values of QMA, UV-Vis absorption spectra of QMA in different pH buffer solutions were recorded, and spectra at several special pH values are shown in Fig.2. Through analysis of these spectral changes with pH variation, four pK_a values of QMA were obtained, and pK_{a1}, pK_{a2}, pK_{a3}, and pK_{a4} are 2.4, 4.2, 5.8, and 8.9, respectively. These pK_a values are assigned to the corresponding sites of QMA (Fig.1). As shown in Scheme 2, there are equilibria between the ionized states, which depend on the pH value of solutions. In different pH ranges, the main ionized state is, $QMAH^+$ (pH<2.4), QMA (2.4−4.2), $QMA[-H^+]^-$ (4.2−5.8), $QMA[-2H^+]^{2-}$ (5.8−8.9), or $QMA[-3H^+]^{3-}$ (pH>8.9), respectively.

B. Molecular conformations of QMA and QME

To obtain the molecular conformations, structures of various ionized-state QMA and QME was optimized and shown in Fig.3. There are two intramolecular hydrogen bonds (H-bonds) in $QMAH^+$ and QMA, one between the nitrogen atom and oxygen atom of the carbonyl group, another between two carboxyl groups. The intramolecular H-bonds create the coplanar conformation of two ionized states, $QMAH^+$ and QMA.

DOI:10.1063/1674-0068/28/cjcp1412217 ©2015 Chinese Physical Society

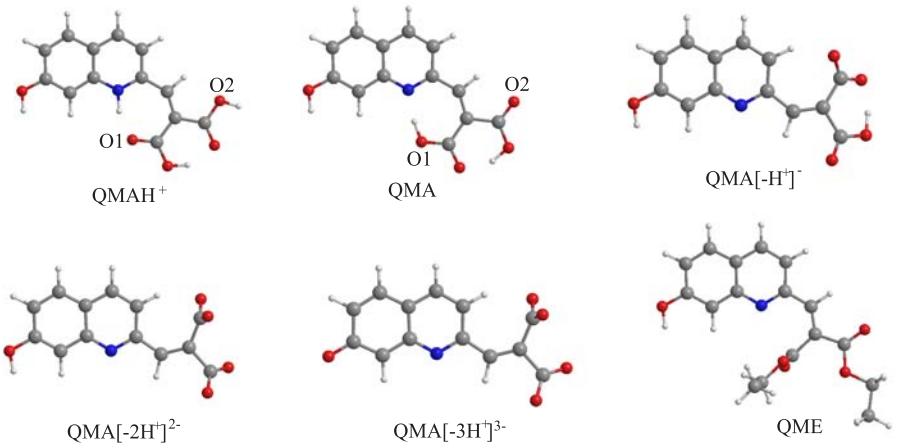

FIG. 3 Optimized structures for five ionized states of QMA and QME.

For this reason, there is a strong conjugation between α, β-unsaturated quinoline and two carbonyl groups in the two ionized states. This conjugation is reflected in their UV-Vis absorption spectra (Fig.2(a)). Two long-band absorption peaks at 338 and 378 nm should be assigned to the two ionized states. As pH value reduces below 2.4, there is only one peak at 338 nm. This may be because the intramolecular H-bond between N−H and oxygen of the carbonyl group is destroyed due to protonation of the carbonyl group in strong acidic solutions. Namely, in very low-pH solutions, there may be only the intramolecular H-bond between two carboxyl groups. The ionized state, QMA[-H^+]$^-$, which exists in slight acidic solutions (pH=4.2−5.8), also has no the long-wavelength absorption peak at 378 nm (Fig.2(b), pH=5.6) due to no existence of the H-bond (NH$\cdots$O), leading to non-coplanar between the quinoline ring and two carboxyl groups (Fig.3). QMA[-2H^+]$^{2-}$ has no intramolecular H-bond, so does the full ionization of QMA forms QMA[-3H^+]$^{3-}$. Calculated structures of the ionized states of QMA are in good agreement with their UV-Vis absorption spectra.

The conformation of QME displays that one ester group is nearly perpendicular to another, and one of them is coplanar with the quinoline ring. This is in agreement with its UV-Vis absorption spectrum that has two peaks of 264 and 323 nm as well as a shoulder at 368 nm (Fig.2(b)).

C. Electrostatic potential maps of QMA and QME

The electrostatic potential map (EPM) can reflect the electrophilicity at a specific position of a molecule. EPMs of four ionized states of QMA as well as QME are listed in Fig.4. The blue color indicates a high potential in a molecule, which implies that the atom at the position has a strong electrophilicity, and the red color reflects a contrary situation. As shown in Fig.3, the electrostatic potentials of α-carbon

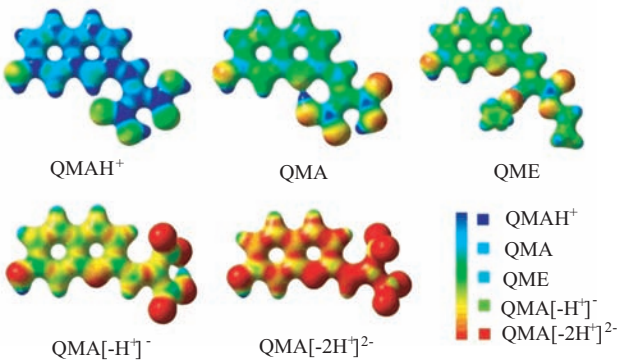

FIG. 4 EPMs and electrostatic potentials at C_α atom for various ionized states of QMA and QME

atom (C_α) in various ionized state are higher than those of β-carbon (C_β). The C_α of QMAH$^+$ has the highest potential, and the lowest potential for QMA[-2H^+]$^{2-}$. The potential of C_α of QME is between QMA and QMA[-H^+]$^-$. These results imply that the electrophilic order of various ionized-state QMA and QME is QMAH$^+$>QMA>QME>QMA[-H^+]$^-$> QMA[-2H^+]$^{2-}$, which should also be the order of the reactivity of a Michael addition. Obviously, as Michael acceptor, QMA is acid-activatable.

D. The sensing mechanism of QMA and QME

1. The sensing mechanism of QMA in acidic solutions

To investigate thermodynamics of the sensing reaction, the reaction of QMAH$^+$ with thioglycolic acid (TGA) in acidic solutions (pH<2.4) was designed as a two-step Michael addition. In the first step, the sulfur of RSH attacks the C_α atom to form S−C bond and a simultaneous proton transfer to oxygen of the carboxyl via initial H-bond to form H−O bond, resulting in an

DOI:10.1063/1674-0068/28/cjcp1412217 ©2015 Chinese Physical Society

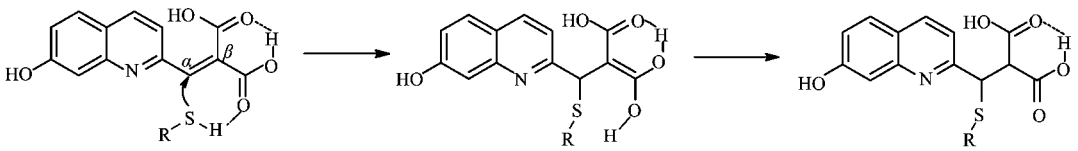

Scheme 3 The proposed acid-activatable Michael addition.

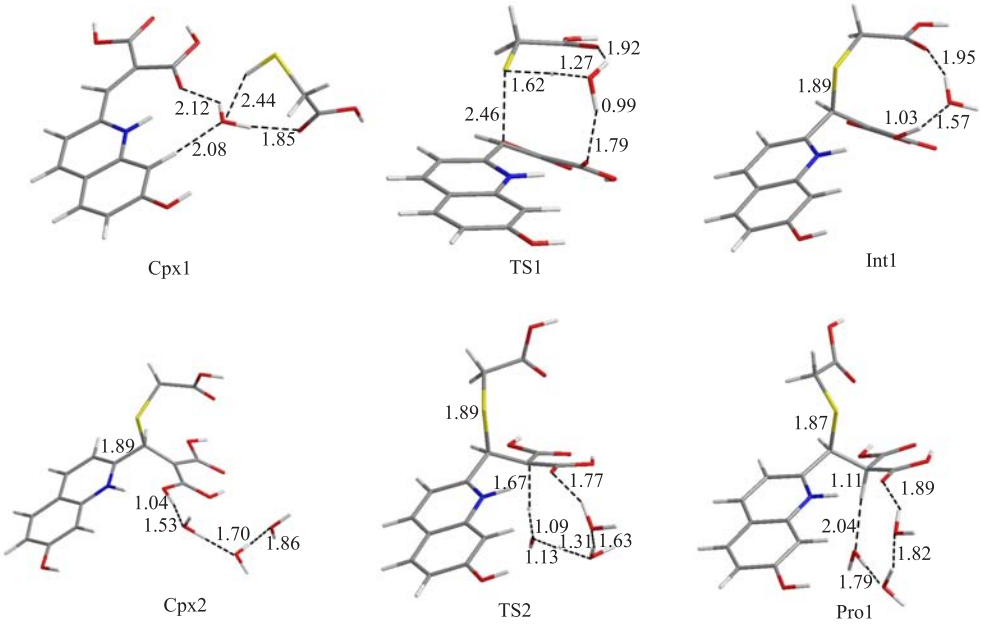

FIG. 5 Complexes and transition states of two-step reaction of $QMAH^+$ with TGA. The bond length is in unit of Å.

enol intermediate. In the second step, the enol undergoes enol-keto tautomerism to afford the adduct, shown in Scheme 3.

One water molecule participates to assist the proton transfer. The complex (Cpx1) of two reactants, $QMAH^+$ and TGA, and one water molecule are stabilized by intermolecular H-bonds. The first step of the reaction is a nucleophilic addition at C_α atom to form an enol intermediate Int1. In the transition state (TS1) of this step, the sulfur atom approaches C_α with a distance of 2.46 Å. The proton of mercapto (-SH) forms a hydrogen bond with water and a proton of water approaches the oxygen of carbonyl group, with a distance of 1.79 Å. Another proton of water forms a hydrogen bond with the carboxyl of TGA, leading to TGA nearly parallel with the carboxyl groups of $QMAH^+$. This step requires an activation enthalpy of 14.8 kcal/mol. In intermediate Int1, the bond length of new H−O is 1.03 Å, the S−C_α is 1.89 Å. This intermediate Int1 is a typical 1,4-addition product. The second-step reaction is the enol-keto tautomerism that Int1 converts into the product (Pro1).

To obtain thermodynamics of this process, two water molecules are introduced to the system. The enol proton transfers to the C_β through three water molecules.

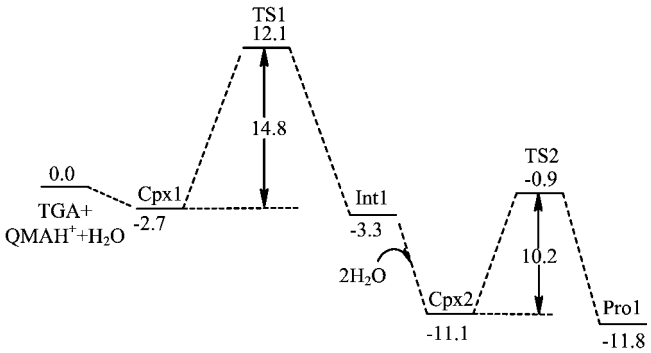

FIG. 6 Enthalpy changes of the reaction relative to individual reactants TGA, $QMAH^+$, and water. Enthalpies are in unit of kcal/mol.

The complex (Cpx2) and transition state (TS2) of this step is shown in Fig.5. This step requires an activation enthalpy of 10.2 kcal/mol, which is lower than the activation enthalpy of the first step. Thus the rate determining step of this two step reaction is the first step. The thermodynamics in the reaction is displayed with enthalpy changes in Fig.6.

Similarly, the sensing process of $QMAH^+$ with Cys

DOI:10.1063/1674-0068/28/cjcp1412217 ©2015 Chinese Physical Society

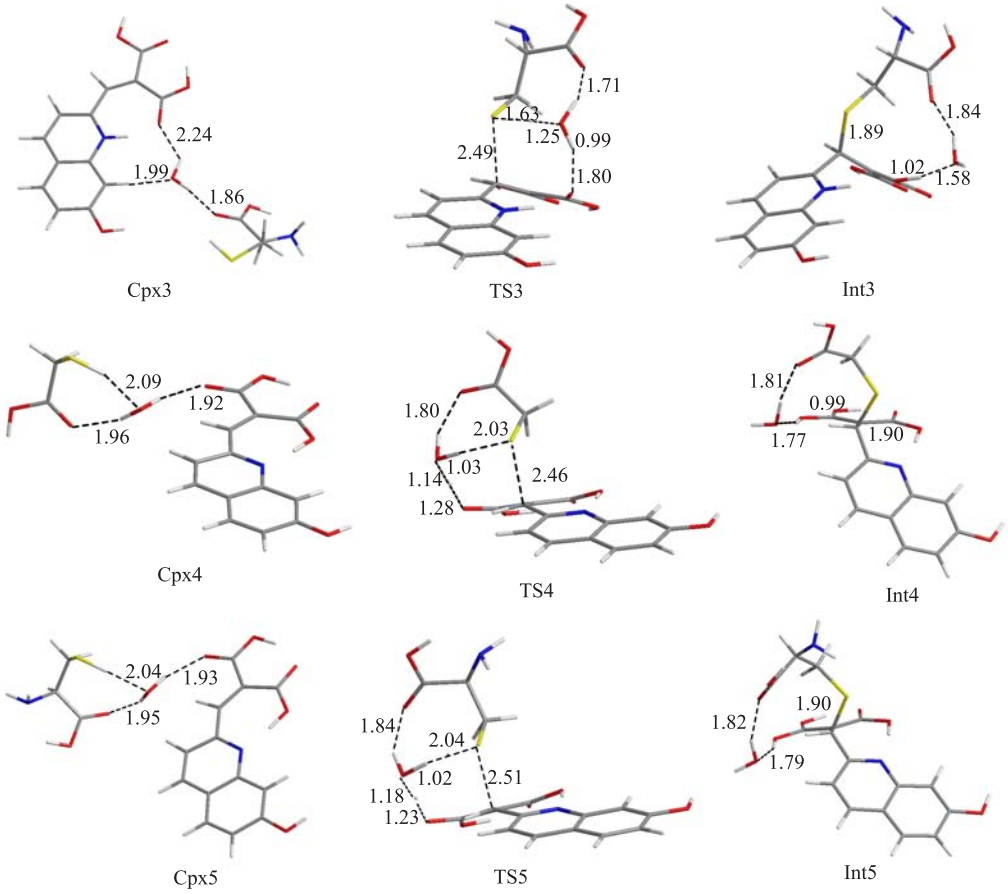

FIG. 7 Complexes and transition states of the first step of the reactions of $QMAH^+$ and Cys (up), QMA and TGA (middle), QMA and Cys (down). The bond length is in unit of Å.

was simulated theoretically. The transition state (TS3) and the intermediate (Int3) in the first step of the reaction is shown in Fig.7. TS3 is similar to TS1. The proton of Cys transfers to the oxygen of carboxyl by a water molecule. Simultaneously, a hydrogen bond is formed between a proton of water and the carboxyl group of Cys. This step requires an activation enthalpy of 12.9 kcal/mol.

In the solutions with pH range of 2.4−4.2, the reaction of QMA with TGA was calculated. The first step is the formation of the enol intermediate Int4 (Fig.7). In the transition state (TS4), the sulfur atom approaches the C_α of QMA, with a distance of 2.46 Å. A proton of water approaches oxygen of carboxyl of QMA, with a short distance of 1.28 Å. This distance is much smaller than that of TS1 due to the deprotonation of carboxyl group. Another proton of water forms a hydrogen bond with the carboxyl of TGA. In contrast to TS1, TGA in TS4 is not parallel with the carboxyl groups of QMA, but toward the opposite side of the carboxyl groups. The corresponding activation enthalpy is 15.4 kcal/mol, which is higher than that of $QMAH^+$ with TGA. Subsequently, Int4 converts to the adduct by an enol-keto tautomerism.

In the pH range of solutions (pH=2.4−4.2), the reaction process of QMA with Cys was simulated, shown in Fig.7. The obtained transition state TS5 is similar to TS4. The activation enthalpy is 16.7 kcal/mol, which is higher than that of the reaction Cys and $QMAH^+$.

In the same way, the reactions of QMA with *n*-propylmercapatan (PM) or cyclohexylmercaptan (CHM) were calculated. Structures of the first-step transition states are shown in Fig.8 and the corresponding activation enthalpies are listed in Table I. Their transition states, TS6 and TS7, are very similar, *i.e.*, they have almost the same lengths of the bonds at the reaction center.

In our previous study [12], second-order rate constants of the reactions between QMA and different thiols in a acidic buffer (pH=3.8) were measured through monitoring UV-Vis absorbance of the reaction system. The second-order rate constants for TGA, PM and CHM are 34.6, 1.9, 1.6 L/(mol·s), respectively. The rate constants for other thiols including homocysteine (Hcy) and glutathione (GSH), 3-mercaptopropanoic acid (MPA) and mercaptoethanol (ME) were further measured and listed in Table S1 in supplementary material. These rate constants are not pK_a-dependent. This

DOI:10.1063/1674-0068/28/cjcp1412217 ©2015 Chinese Physical Society

TABLE I Structures and activation enthalpies of first-step transition states in reactions of QMA or QME with thiols[a].

Entry	Form of reactants		Energies of TS/(kcal/mol)			k_2/(L/(mol·s))
	Probe	Thiols	R−S$\cdots$C$_\alpha$	R−S$\cdots$H$\cdots$O$\cdots$H$\cdots$O	$\Delta H^{\neq}$	
1	QMAH$^+$	TGA	2.46	1.62, 1.27, 0.99, 1.79	14.8	
2	QMAH$^+$	Cys	2.49	1.63, 1.25, 0.99, 1.80	12.9	
3	QMA	TGA	2.46	2.04, 1.03, 1.14, 1.28	15.4	34.6
4	QMA	Cys	2.51	2.04, 1.03, 1.18, 1.23	16.7	5.4
5	QMA	PM	2.51	1.77, 1.13, 1.14, 1.29	15.6	1.9
6	QMA	CHM	2.53	1.78, 1.12, 1.14, 1.28	16.9	1.6
7[b]	QMA[-H$^+$]$^-$	TGA[-H$^+$]$^-$	2.47	1.61, 1.28	19.7	
8[b]	QMA[-2H$^+$]$^{2-}$	TGA[-H$^+$]$^-$	2.32	2.17, 1.00	26.2	
9[b]	QMA[-2H$^+$]$^{2-}$	TGA[-2H$^+$]$^{2-}$	2.08		34.3	
10	QME	PM[-H$^+$]$^-$	2.40	2.53, 0.98, 0.98, 1.98	4.4	4.6
11	QME	PM	1.91	1.61, 1.26, 1.09, 1.37	21.8	
12	QME	Cys[-2H$^+$]$^{2-}$	2.61	2.56, 0.98, 0.98, 1.98	4.4	73.6
13	QME	Cys	1.97	1.55, 1.35, 1.01, 1.63	23.2	

[a] The values of $\Delta H^{\neq}$ relative to their corresponding complexes unless other indicate.
[b] Related to individule reactants.

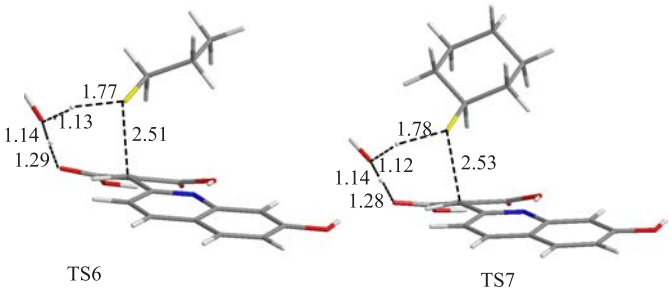

FIG. 8 Transition states of the reaction of QMA with PM (left) or CHM (right). The bond length is in unit of Å.

implies that thiols in their neutral forms participate in the sensing reaction. Calculated activation enthalpies for these reaction systems support their rate constants from experimental measurements (Table I).

In addition, in slight acidic solutions (pH=4.2−5.8), the ionized state of QMA and TGA are QMA[-H$^+$]$^-$ and TGA[-H$^+$]$^-$ respectively. Calculation result displays that the reaction of QMA[-H$^+$]$^-$ with TGA[-H$^+$]$^-$ has a bit high activation energy, $\Delta H^{\neq}$=19.7 kcal/mol (Fig.9), which supports low reactivity of QMA with Cys in this pH range of 4.2−5.8.

2. The interaction of QMA with thiols in alkaline solutions

In neutral and slight alkaline solutions (pH=5.8−8.9), the ionized state, QMA[-2H$^+$]$^{2-}$, doesn't have the intramolecular H-bond. TGA[-H$^+$]$^-$ and TGA[-2H$^+$]$^{2-}$ as anion forms of TGA exist in the solutions. The transition states (TS9, TS10) of reactions of QMA[-2H$^+$]$^{2-}$ with TGA[-H$^+$]$^-$ or TGA[-2H$^+$]$^{2-}$, are shown in Fig.9. Two water molecules were added to disperse the negative charge of carboxylate of QMA[-2H$^+$]$^{2-}$. The distances between the sulfur atom and the C$_\alpha$ are 2.32 Å for TGA[-H$^+$]$^-$ and 2.08 Å for TGA[-2H$^+$]$^{2-}$. The complexes of two reactions were not obtained. By comparing the energy of TS9 or TS10 with the sum of the two reactants, the activation enthalpies were obtained, 26.2 kcal/mol for TS9 and 34.3 kcal/mol for TS10. These $\Delta H^{\neq}$ values imply that the processes are difficult to occur in neutral and slight alkaline solutions.

3. The sensing mechanism of QME

In contrast, QME, the ester of QMA, doesn't have various ionized states like QMA in a near neutral pH range (pH=4−9). However, there is a ionization equilibrium between RSH and its thiolate anion RS$^-$ for thiols. The nucleophilicity of RS$^-$ is stronger than that of the RSH. The deprotonated PM and Cys were chosen as nucleophiles. The ionized states, PM[-H$^+$]$^-$ and Cys[-2H$^+$]$^{2-}$, are fixed upon the C$_\alpha$=C$_\beta$ bond of QME in their complexes Cpx11 and Cpx12 (Fig.10), with a distance of 3.05 Å to the C$_\alpha$ of QME. In Cpx11, one water molecule was added near the carbonyl group coplanar with the quinoline ring. The distance between a proton of water and the sulfur atom is 2.41 Å and the distance between another proton and the oxygen of carbonyl group is 2.09 Å. The sulfur atom approaches the C$_\alpha$ of QME and forms the transition state TS11, in which the distance between the sulfur atom and C$_\alpha$ (S-C$_\alpha$) is 2.40 Å. The water molecule slightly depart from PM[-H$^+$]$^-$ and approaching QME. The structure of TS11 is similar to Cpx11, *i.e.*, an early transition state. The formation of the intermediate Int11 requires

DOI:10.1063/1674-0068/28/cjcp1412217 ©2015 Chinese Physical Society

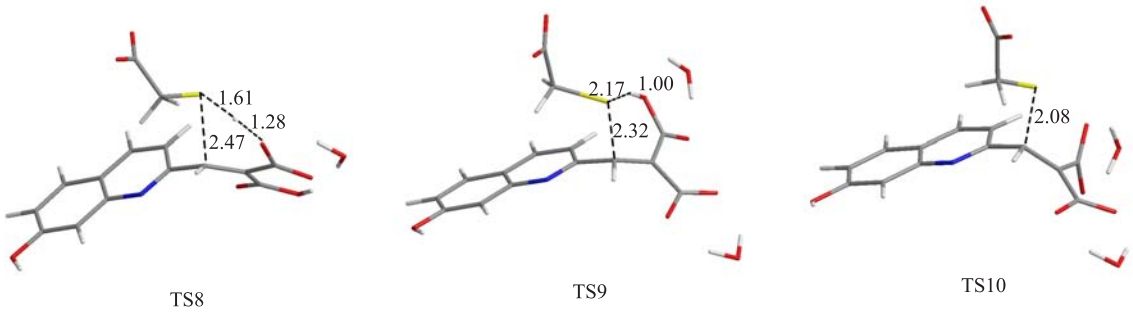

FIG. 9 Structures of transition states of the reaction of QMA[-H^+]$^-$ or QMA[-$2H^+$]$^{2-}$ with TGA[-H^+]$^-$ and QMA[-$2H^+$]$^{2-}$ with TGA[-$2H^+$]$^{2-}$. The bond length is in unit of Å.

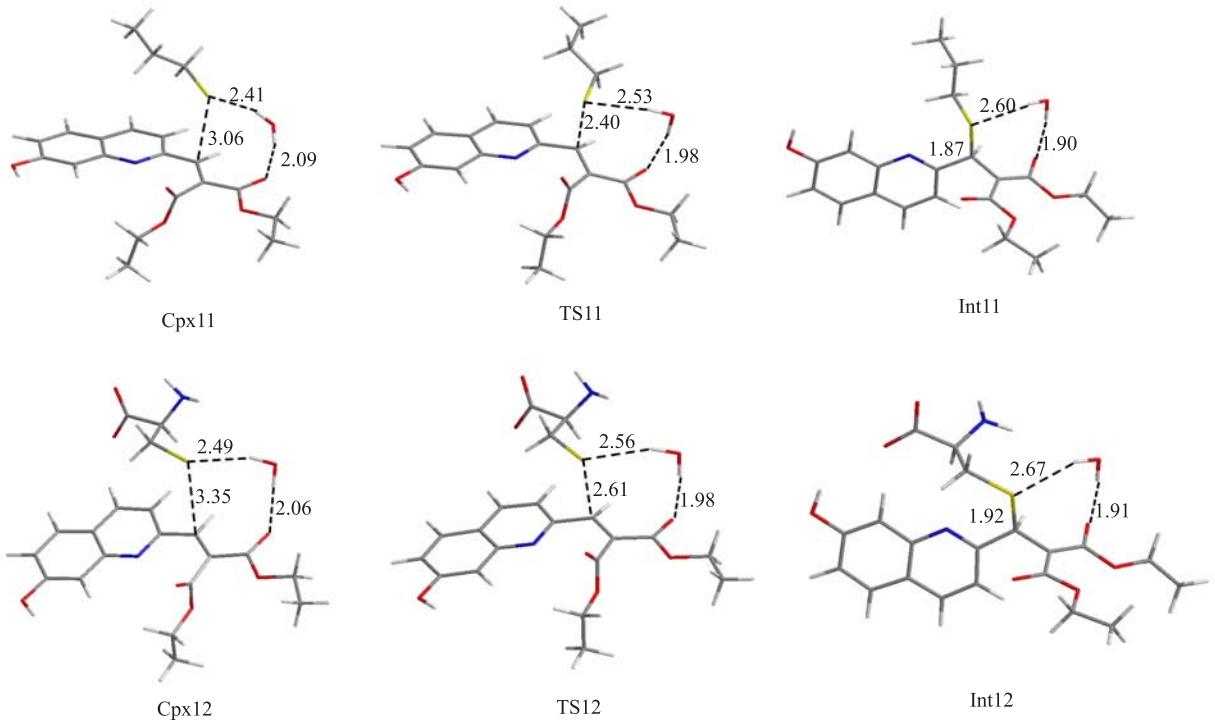

FIG. 10 Structures of complexes, transition states and intermediates of the reaction of QME with PM[-H^+]$^-$ (up) or Cys[-$2H^+$]$^{2-}$ (down). The bond length is in unit of Å.

a low activation enthalpy of 4.4 kcal/mol. In Int11, the water molecule is further apart from the sulfur atom and approaches the carbonyl group. The bond length of S−C_α is 1.88 Å. Finally, the carbanion at C_β is fast protonated to form Pro11. This is a 1,2-addition process.

To examine the possibility of the reaction between QME and thiols in slight acidic solutions such as solutions with pH range of 4−6, neutral form of QME (Cys and PM) and thiols were chosen to be reactants and their reactions were monitored. The complexes Cpx13, Cpx14 and transition states TS13, TS14 of reactions are shown in Fig.11. Their activation enthalpies are high, 23.2 kcal/mol for Cys and 21.8 kcal/mol for PM.

As shown in Table I, the reactions of the same ionized-state QMA with similar thiols (such as TGA and Cys, PM and CHM) result in similar structures of the reaction centre in transition states. The C_α−S distances in TS are 2.46−2.53 Å for entry 1−7 and 2.32, 2.08 for entry 8 and entry 9. The former is early TS with a low activation energy, and the latter is later TS with a high activation energy. Moreover, comparison of structures of TS clearly shows an early TS for QME-PM[-H^+]$^-$ system and a later TS for QME-PM system (entry 10 and entry 11 in Table I).

IV. DISCUSSION

QMA is a multiple ionized-state molecule, its form is pH-dependent. There are equilibria between various ionized states. Based on measured pK_a val-

DOI:10.1063/1674-0068/28/cjcp1412217 ©2015 Chinese Physical Society

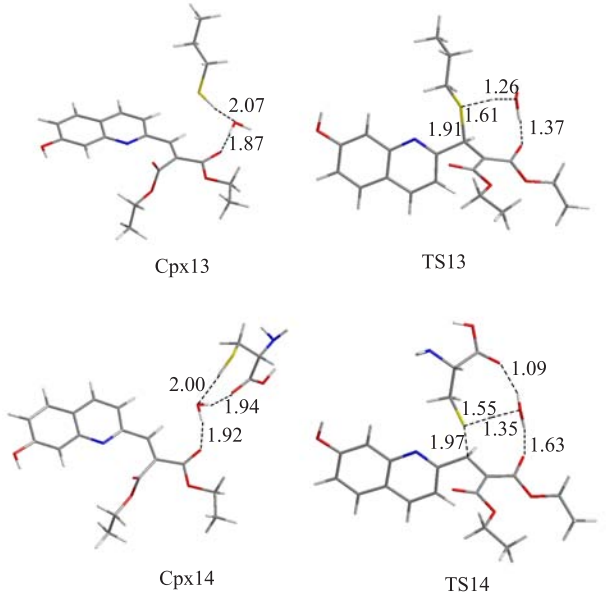

FIG. 11 Complexes and transition states of systems of QME with PM (up) or Cys (down). The bond length is in unit of Å.

ues, main ionized state in the pH range of solutions is $QMAH^+$(pH<2.4), QMA (2.4−4.2), $QMA[-H^+]^-$ (4.2−5.8), $QMA[-2H^+]^{2-}$ (5.8−8.9) or $QMA[-3H^+]^{3-}$ (pH> 8.9), respectively. The electrostatic potentials for various ionized states of QMA from quantum chemical calculation display that the order of electrostatic potential at C_α atom is $QMAH^+$>QMA>QME>$QMA[-H^+]^-$>$QMA[-2H^+]^{2-}$, and higher at C_α atom over C_β atom for the same molecule/ion. Namely, in the lower pH solution, QMA is more highly electrophilic Michael acceptor, that is, QMA is acid-activatable.

In several pH ranges, thermodynamic calculations of the sensing reaction of reactants in the corresponding ionized state reveal an activation-enthalpy order of $QMAH^+$>QMA>$QMA[-H^+]^-$> $QMA[-2H^+]^{2-}$ with the same thiol (Table I). In acidic solutions, the form of thiols is RSH, and thiolate anion RS^- in alkaline solutions. The order of activation energies ($\Delta H^{\neq}$) accords to second-order rate constants from experimental measurements (Table I and Table S1). The values of rate constants in pH=3.8 solution display to be independent of pK_α values of thiols, *i.e.*, in the acidic solution, the probe reacts with RSH rather than RS^-.

As shown in Table I, the structures of transition states display that the bond length of S−C_α are longer in acidic solutions (entry 1−7 in Table I) over alkaline solutions (entry 8 and 9) for QMA systems, while QME has a contrary pH effect, *i.e.*, the distance of S−C_α is longer in alkaline solutions (entry 10 and 12) over acidic solutions (entry 11 and 13). It indicates an earlier TS for the systems of QMA with RSH in acidic solutions, and later TS for the QMA system with RS^- in alkaline solutions, while QME is converse.

For the sensing reaction process, the Michael donor RSH adds to the acceptor QMA via 1,4-addition. The sulfur atom of RSH attacks nucleophilically the C_α of QMA and protonation occurs at oxygen of carbonyl group, yielding an enol which would rapidly ketonize. In contrast, in alkaline solutions, QME is attacked nucleophilically by thiolate anion RS^- via 1,2-addition. The nucleophile RS^- adds to C_α atom of QME and final protonation occurs at C_β atom.

Finally, we compare the sensing reactions of two kinds of thiol probes QMA and QME. Firstly, the reactivity order of probes as Michael acceptors was obtained based on calculation of electrostatic potentials for various ionized-state QMA and QME. Secondly, two probes display contrary pH effects on the sensing reactivity, resulting in two pH-working ranges, pH<7 for QMA and pH>7 for QME. Correspondingly, the Michael donor is RSH for QMA, and RS^- for QME. Thirdly, the sensing reaction of QMA undergoes a 1,4-addition, and 1,2-addition for QME. Lastly, the activation energy of QME with RS^- is lower than that of QMA with RSH. However, this doesn't imply that the former rate is higher than the latter as the concentration of RS^- is very low in a slight alkaline solution.

V. CONCLUSION

In summary, we demonstrated that the sensing mechanism of novel acid-activatable probes, QMA, which works in acidic conditions (pH<7), and compared to their esters, QME, which works in alkaline conditions (pH>7), by experimental study and theoretic calculation. The pK_a values measured from UV-Vis absorption spectra of QMA in different pH solutions show that various ionized states of QMA exist in the corresponding pH range of solutions. The calculation results display that the order of their reactivity is $QMAH^+$>QMA>QME>$QMA[-H^+]^-$> $QMA[-2H^+]^{2-}$, *i.e.*, the lower pH value of solution, the sensing reactivity is higher. In acidic solutions, the highly reactive ionized states ($QMAH^+$, QMA) can react with RSH undergoing a 1,4-addition process. However, lowly reactive $QMA[-2H^+]^{2-}$ cannot react with both RSH and RS^- due to a high-energy transition state. In contrast, the reaction of QME with RS^- is low-energy-barrier process in alkaline solution via a 1,2-addition, while QME cannot react with RSH in acidic solutions. The geometrical bond-length changes of TS and activation enthalpies are in good agreement with experimental results such as pH effects on the sensing reactivity for QMA and QME, and their second-order rate constants.

Supplementary material: Analytical and spectral characterization data, computational details and structures of complexes, transition states, intermediates and products are given.

DOI:10.1063/1674-0068/28/cjcp1412217 ©2015 Chinese Physical Society

VI. ACKNOWLEDGMENTS

This work is supported by the National Natural Science Foundation of China (No.21272224), the Open Research Fund of State Key Laboratory of Physical Chemistry of Solid Surfaces, Xiamen University (No.201410), and the Open Research Fund of Key Laboratory of Advanced Scientific Computation, Xihua University (No.szjj2013-024).

[1] (a) S. Y. Zhang, C. N. Ong, and H. M. Shen, Cancer Lett. **208**, 143 (2004).
(b) K. S. Jensen, R. E. Hansen, and J. R. Winther, Antioxid. Redox Signaling **11**, 1047 (2009).
[2] (a) G. Wu, Y. Z. Fang, J. R. Lupton, and N. D. Turner, J. Nutr. **134**, 489 (2004).
(b) T. P. Dalton, H. G. Shertzer, and A. Puga, Annu. Rev. Pharmacol. Toxicol. **39**, 67 (1999).
(c) S. M. Kanzok, R. H. Schirmer, I. Turbachova, R. Lozef, and K. Beeker, J. Biol. Chem. **275**, 40180 (2000).
[3] S. Shahrokhian, Anal. Chem. **73**, 5972 (2001).
[4] S. Seshadri, A. Beiser, J. Selhub, P. F. Jacques, I. H. Rosenberg, R. B. D'Agostino, P. W. F. Wilson, and P. A. N. Wolf, Engl. J. Med. **346**, 476 (2002).
[5] (a) X. Chen, Y. Zhou, X. Peng, and J. Yoon, Chem. Sov. Rev. **39**, 2120 (2010).
(b) E. M. Maria, R. Matínez-Máñez, and F. Sancenón, Chem. Sov. Rev. **40**, 2593 (2011).
(c) K. Kaur, R. Saini, A. Kumar, V. Luxami, N. Kaur, P. Singh, and S. Kumar, Coord. Chem. Rev. **256**, 1992 (2012).
[6] (a) V. Hong, A. A. Kislukhin, and M. G. Finn, J. Am. Chem. Soc. **131**, 9986 (2009).
(b) F. J. Huo, Y. Q. Sun, J. Su, J. B. Chao, H. J. Zhi, and C. X. Yin, Org. Lett. **11**, 4918 (2009).
(c) L. Yi, H. Li, L. Sun, L. Liu, C. Zhang, and Z. Xi, Angew. Chem. Int. Ed. **48**, 4034 (2009).
(d) W. Lin, L. Yuan, Z. Cao, Y. Feng, and L. Long, Chem. Eur. J. **15**, 5096 (2009).
(e) S. Lim, J. O. Escobedo, M. Lowry, X. Xu, and R. Strongin, Chem. Commun. **46**, 5707 (2010).
(f) Q. Zuo, B. Li, Q. Pei, Z. Li, and S. Liu, J. Fluoresc. **20**, 1307 (2010).
(g) H. Kwon, K. Lee, and H. Kim, Chem. Commun. **47**, 1773 (2011).
(h) H. S. Lung, K. C. Ko, G. Kim, A. Lee, Y. Na, C. Kang, J. Y. Lee, and J. S. Kim, Org. Lett. **13**, 1498 (2011).
(i) G. Kim, K. Lee, H. Kwon, and H. Kim, Org. Lett. **13**, 2799 (2011).
(j) L. Yuan, W. Lin, and Y. Yang, Chem. Commun. **47**, 6275 (2011).
(k) Y. Q. Sun, M. Chen, J. Liu, X. Lv, J. F. Li, and W. Guo, Chem. Commun. **47**, 11029 (2011).
(l) A. Lim and H. Kim, Tetrahedron Lett. **52**, 3189 (2011).
(m) H. J. Ha, D. H. Yoon, S. Park, and H. J. Kim, Tetrahedron. **67**, 7759 (2011).
(n) L. Deng, W. Wu, H. Guo, J. Zhao, S. Ji, X. Zhang, X. Yuan, and C. Zhang, J. Org. Chem. **76**, 9294 (2011).
(o)J. Du, Z. Yang, H. Qi, and X. F. Yang, Luminescence **26**, 486 (2011).
(p) D. Kand, A. M. Kalle, S. J. Varma, and P. Talukdar, Chem. Commun. **48**, 2722 (2012).
(q) H. S. Jung, J. H. Han, T. Pradhan, S. Kim, S. W. Lee, J. L. Sessler, T. W. Kim, C. Kang, and J. S. Kim, Biomaterials **33**, 945 (2012).
(r) S. Madhu, R. Gonnade, and M. Ravikanth, J. Org. Chem. **78**, 5056 (2013).
(s) M. Isik, T. Ozdemir, I. S. Turan, S. Kolemen, and E. U. Akkaya, Org. Lett. **15**, 216 (2013).
(t) Y. T. Yang, F. J. Huo, C. X. Yin, A. M. Zheng, J. B. Chao, Y. Q. Li, Z. X. Nie, R. Martínez-Máñez, and D. S. Liu, Biosensors Bioelectronics **47**, 300 (2013).
(u) T. Miyoshi, Y. Aoki, Y. Uno, M. Araki, T. Kamatani, D. Fujii, Y. Fujita, N. Takeda, M. Ueda, H. Kitagawa, N. Emoto, T. Mukai, M. Tanaka, and O. Miyata, J. Org. Chem. **78**, 11433 (2013).
(v) L. L. Long, L. P. Zhou, L. Wang, S. C. Meng, A. H. Gong, F. Y. Du, and C. Zhang, Org. Biomol. Chem. **11**, 8214 (2013).
(w) H. S. Jung, X. Q. Chen, J. S. Kim, and J. Y. Yoon, Chem. Soc. Rev. **42**, 6019 (2013).
(x) A. Agostini, I. Campos, M. Milani, S. Elsayed, L. Pascual, R. Martínez-Máñez, M. Licchelli, and F. Sancenón, Org. Biomol. Chem. **12**, 1871 (2014).
[7] (a) J. H. Lee, C. S. Lim, Y. S. Tian, J. H. Han, and B. R. Cho, J. Am. Chem. Soc. **132**, 1216 (2010).
(b) W. Jiang, Y. T. Cao, Y. Liu, and W. Wang, Chem. Commun. **46**, 1944 (2010).
(c) W. Y. Lin, L. L. Long, and W. Tan, Chem. Commun. **46**, 1503 (2010).
(d) X. Li, S. Qian, Q. He, B. Yang, J. Li, and Y. Hu, Org. Biomol. Chem. **8**, 3627 (2010).
(e) C. C. Zhao, Y. Zhou, Q. N. Lin, L. Y. Zhu, P. Feng, Y. L. Zhang, and J. Cao, J. Phys. Chem. B **115**, 642 (2011).
(f) J. Shao, H. Sun, H. Guo, S. Ji, J. Zhao, W. Wu, X. Yuan, C. Zhang, and T. D. James, Chem. Sci. **3**, 1049 (2012).
(g) X. D. Jiang, J. Zhang, X. Shao, and W. Zhao, Org. Biomol. Chem. **10**, 1966 (2012).
(h) X. L. Liu, X. Y. Duan, X. J. Du, and Q. H. Song, Chem. Asian J. **7**, 2969 (2012).
(i) Z. C. Dai, L. Tian, Z. Q. Ye, B. Song, R. Zhang, and J. Yuan, Anal. Chem. **85**, 11658 (2013).
(j) M. J. Wei, P. Yin, Y. M. Shen, L. L. Zhang, J. H. Deng, S. Y. Xue, H. T. Li, B. Guo, Y. Y. Zhang, and S. Z. Yao, Chem. Commun. **49**, 4640 (2013).
(k) S. Chen, P. Hou, B. J. Zhou, X. Z. Song, J. S. Wu, H. Y. Zhang, and J. W. Foley, RSC Adv. **3**, 11543 (2013).
(l)J. Li, C. F. Zhang, Z. Z. Ming, W. C. Yang, and G. F. Yang, RSC Adv. **3**, 26059 (2013).
(m) H. S. Jung, X. Q. Chen, J. S. Kim, and J. Y. Yoon, Chem. Soc. Rev. **42**, 6019 (2013).
(n) M. Li, X. M. Wu, Y. Wang, Y. S. Li, W. H. Zhu, and T. D. James, Chem. Commun. **50**, 1751 (2014).
[8] (a) Z. Yao, X. Feng, C. Li, and G. Shi, Chem. Commun. 5886 (2009).
(b) H. Lin, J. Fan, J. Wang, M. Tian, J. Du, S. Sun, P. Sun, and X. Peng, Chem. Commun. 5904 (2009).
(c) H. Hu, J. Fan, H. Li, K. Song, S. Wang, G. Chen,

DOI:10.1063/1674-0068/28/cjcp1412217 ©2015 Chinese Physical Society

and X. Peng, Org. Biomol. Chem. **9**, 980 (2011).
(d) J. Mei, J. Tong, J. Wang, A. Qin, J. Z. Sun, and B. Z. Tang, J. Mater. Chem. **22**, 17063 (2012).
(e) Z. Yang, N. Zhao, Y. Sun, F. Miao, Y. Liu, X. Liu, Y. Zhang, W. Ai, G. Song, X. Shen, X. Yu, J. Sun, and W. Y. Wong, Chem. Commun. **48**, 3442 (2012).
(f) H. J. Lee and H. J. Kim, Org. Biomol. Chem. **11**. 5012 (2013).
(g) F. P. Kong, R. P. Liu, R. R. Chu, X. Wang, K. H. Xu, and B. Tang, Chem. Commun. **49**, 9176 (2013).

[9] (a) J. Wu, R. Sheng, W. Liu, P. Wang, J. Ma, H. Zhang, and X. Zhuang, Inorg. Chem. **50**, 6543 (2011).
(b) B. Ma, F. Zeng, X. Li, and S. Wu, Chem. Commun. **48**, 6007 (2012).
(c) T. T. Zou, C. T. Lum, S. S. Chui, and C. M. Che, Angew. Chem. Int. Ed. **52**, 2930 (2013).
(d) R. X. Peng, L. L. Lin, X. X. Wu, X. H. Liu, and X. M. Feng, J. Org. Chem. **78**, 11602 (2013).

[10] (a) H. S. Hewage and E. V. Anslyn, J. Am. Chem. Soc. **131**, 13099 (2009).
(b) N. Shao, J. Jin, H. Wang, J. Zheng, R. Yang, W. Chan, and Z. Abliz, J. Am. Chem. Soc. **132**, 725 (2010).
(c) L. Long, W. Lin, B. Chen, W. Chao, and L. Yuan, Chem. Commun. **47**, 893 (2011).
(d) Z. Guo, S. W. Nam, S. Park, and J. Yoon, Chem. Sci. **3**, 2760 (2012).
(e) L. Y. Niu, Y. S. Guan, Y. Z. Chen, L. Z. Wu, C. H. Tung, and Q. Z. Yang, J. Am. Chem. Soc. **134**, 18928 (2012).
(f) B. C. Zhu, Y. Z. Zhao, Q. Zhou, B. Zhang, L. Y. Liu, B. Du, and X. L. Zhang, Eur. J. Org. Chem. **5**, 888 (2013).
(g) Y. S. Guan, L. Y. Niu, Y. Z. Chen, L. Z. Wu, C. H. Tung, and Q. Z. Yang, RSC Adv. **4**, 8360 (2014).

[11] (a) W. Zhao, W. Liu, J. Ge, J. Wu, W. Zhang, X. Meng, and P. Wang, J. Mater. Chem. **21**, 13561 (2011).
(b) J. W. Nielsen, K. S. Jensen R. E. Hansen, C. H. Gotfredsen, and J. R. Winther, Anal. Biochem. **421**, 115 (2012).

[12] Q. H. Song, Q. Q. Wu, C. H. Liu, X. J. Du, and Q. X. Guo, J. Mater. Chem. B **1**, 438 (2013).

[13] M. J. Frisch, G. W. Trucks, H. B. S chlegel, G. E. Scuseria, M. A. Robb, J. R. Cheeseman, G. Scalmani, V. Barone, B. Mennucci, G. A. Petersson, H. Nakatsuji, M. Caricato, X. Li, H. P. Hratchian, A. F. Izmaylov, J. Bloino, G. Zheng, J. L. Sonnenberg, M. Hada, M. Ehara, K. Toyota, R. Fukuda, J. Hasegawa, M. Ishida, T. Nakajima, Y. Honda, O. Kitao, H. Nakai, T. Vreven, J. A. Jr. Montgomery, J. E.Peralta, F. Ogliaro, M. Bearpark, J. J. Heyd, E. Brothers, K. N. Kudin, V. N. Staroverov, R. Kobayashi, J. Normand, K. Raghavachari, A. Rendell, J. C. Burant, S. S. Iyengar, and J. Tomasi, *Gaussian 09, ReVision A.02*, Wallingford, CT: Gaussian, Inc., (2009).

DOI:10.1063/1674-0068/28/cjcp1412217 ©2015 Chinese Physical Society